Surface Interactome in *Streptococcus pyogenes*[*][S]

Cesira L. Galeotti‡, Elia Bove‡, Alfredo Pezzicoli‡, Renzo Nogarotto‡§, Nathalie Norais‡, Silvia Pileri¶, Barbara Lelli¶, Fabiana Falugi‡, Sergio Balloni‡, Vittorio Tedde‡, Emiliano Chiarot‡, Mauro Bombaci‡‖, Marco Soriani‡, Luisa Bracci¶, Guido Grandi‡, and Renata Grifantini‡§**

Very few studies have so far been dedicated to the systematic analysis of protein interactions occurring between surface and/or secreted proteins in bacteria. Such interactions are expected to play pivotal biological roles that deserve investigation. Taking advantage of the availability of a detailed map of surface and secreted proteins in *Streptococcus pyogenes* (group A *Streptococcus* (GAS)), we used protein array technology to define the "surface interactome" in this important human pathogen. Eighty-three proteins were spotted on glass slides in high density format, and each of the spotted proteins was probed for its capacity to interact with any of the immobilized proteins. A total of 146 interactions were identified, 25 of which classified as "reciprocal," namely, interactions that occur irrespective of which of the two partners was immobilized on the chip or in solution. Several of these interactions were validated by surface plasmon resonance and supported by confocal microscopy analysis of whole bacterial cells. By this approach, a number of interesting interactions have been discovered, including those occurring between OppA, DppA, PrsA, and TlpA, proteins known to be involved in protein folding and transport. These proteins, all localizing at the septum, might be part, together with HtrA, of the recently described ExPortal complex of GAS. Furthermore, SpeI was found to strongly interact with the metal transporters AdcA and Lmb. Because SpeI strictly requires zinc to exert its function, this finding provides evidence on how this superantigen, a major player in GAS pathogenesis, can acquire the metal in the host environment, where it is largely sequestered by carrier proteins. We believe that the approach proposed herein can lead to a deeper knowledge of the mechanisms underlying bacterial invasion, colonization, and pathogenesis. ***Molecular & Cellular Proteomics 11: 10.1074/mcp.M111.015206, 1–13, 2012.***

From the ‡Novartis Vaccines, Via Fiorentina 1, 53100 Siena, Italy and the ¶Department of Molecular Biology, University of Siena, Via Fiorentina 1, 53100, Siena, Italy

Received October 18, 2011
Published, MCP Papers in Press, December 22, 2011, DOI 10.1074/mcp.M111.015206

Surface proteins play a fundamental role in bacterial adaptation, survival, and proliferation. They sense the chemical and physical conditions of the external environment and send appropriate signals to the cytoplasmic compartment, control the in/out trafficking of a plethora of molecules and ions, serve as anchoring tools for adhesion, and promote biofilm formation. In pathogenic bacteria, they also participate in tissue colonization and invasion and contribute considerably to counteract the defense mechanisms of the host. As a consequence of their role in key biological processes, surface protein identification has become instrumental not only for the definition of the mechanisms underlying bacterial physiology and pathogenesis but also for the development of new antimicrobial therapeutic and prophylactic products.

The precise elucidation of bacterial surface proteomes ("surfome") is experimentally challenging. Contamination of the surface/membrane protein preparations with cytoplasmic proteins can prevent accurate proteome characterization both in qualitative and quantitative terms. Furthermore, functionally important complexes that may form on the bacterial surface can remain largely undetected because the experimental conditions used for sample preparation and analysis usually destroy noncovalent protein-protein interactions.

In the last few years, new effective protocols for the identification and quantification of surface-associated proteins have been developed. They include *in silico* analysis of genome sequences combined with the use of antibodies specific for each predicted surface protein to confirm its surface exposure on whole bacterial cells (1–4), *in vivo* labeling of surface proteins coupled to mass spectrometry (5), protease "shaving" of bacterial surfaces and analysis of proteolytic peptides by mass spectrometry (6–9), and mass spectrometry analysis of outer membrane vesicles (10, 11).

In regard to the identification of surface protein complexes, several experimental methods exist (12), the most commonly used being the yeast two-hybrid system (13, 14), the tandem affinity purification (tagging) approach combined with protein identification using mass spectrometry (15, 16) and protein microarray (17, 18). However, none of them have so far been exploited to decipher the interactions taking place at the bacterial surface. Therefore, whereas the number of bacterial

"surfomes" determined with a sufficiently high degree of accuracy is growing, the characterization of "surface interactomes" remains a field almost completely unexplored.

The aim of this study is to further our understanding of this field. Using *Streptococcus pyogenes* (group A *Streptococcus* (GAS))[1] as a model system and taking advantage of the availability of its surfome at a good level of resolution (6),[2] protein arrays of 83 surface-exposed proteins have been produced. The ability of these proteins to form complexes has then been investigated by probing the array with biotin-labeled derivatives of each of the spotted proteins. Some of the identified interactions have been validated by determining the kinetic and thermodynamic constants of interactions using surface plasmon resonance and by demonstrating co-localization of some the interacting proteins on the bacterial surface by confocal microscopy. Overall, the approach has unraveled a network of interactions taking place at the surface of GAS, interactions that might explain some fundamental mechanisms of the biology and virulence of this important human pathogen.

EXPERIMENTAL PROCEDURES

Selection of GAS Surface Proteins—Computer programs included in the GCG Wisconsin Package version 11.1, in combination with the PSORT program, were used to analyze the sequences from different GAS strains. A subset of predicted surface-associated proteins was selected from the analysis of the genome of *S. pyogenes* strain SF370, with the exception of SpyM3_0104 (nomenclature and sequences based on MGAS315) that was selected from strain 3040 (M3); SpyM6_0157 (nomenclature and sequence from MGAS10394) selected from strain 2724 (M6); and gi-19224134 and gi-19224141 (nomenclature and sequence from A715) selected from strain 2728 (M12).

Cloning and Protein Purification—After PCR amplification, genomic DNA coding for the mature portion of the selected proteins was cloned into the pET21b expression vector (Novagen) using *Escherichia coli* BL21(DE3) as a host (Novagen). Recombinant proteins, obtained as C-terminal His tag fusions, were purified using an automated AKTAxpress system on a nickel affinity column, followed by a desalting step and an ion exchange column (19). Proteins purified in a tagless form were obtained as described by Klock *et al.* (20). Briefly, the PCR product of the portion of the gene coding for the mature protein was cloned into plasmid pSpeedET, which encodes an expression and purification tag followed by a tobacco etch virus protease site (MGSDKIHHHHHHENLYFQG) at the N terminus of the protein. Protein expression was performed in an arabinose-containing medium using the *E. coli* strain HK100 [F− mcrA (mrr-hsdRMS-mcrBC) 80lacZM15 lacX74 recA1 endA1 araΔ139 (ara-leu)7697 galU galK rpsL(StrR) nupG]. At the end of growth, lysozyme was added to the culture to a final concentration of 1 mg/ml, and the cells were harvested. After one freeze/thaw cycle, the cells were lysed in B-PER Buffer (bacterial protein extraction reagent; Pierce), and the lysate was clarified by centrifugation at 35,000 × *g* for 30 min. The soluble fraction was loaded onto a nickel-chelating resin pre-equilibrated with wash buffer (300 mM NaCl, 50 mM sodium phosphate, pH 8.0). The resin was washed with wash buffer containing 20 mM imidazole, and the protein was eluted with the same buffer containing 500 mM imidazole. The eluate was buffer exchanged with HEPES buffer (50 mM HEPES, pH 8.0, 1 mM tris(2-carboxyethyl)phosphine) using a HighTrap desalting column and digested with 1 mg of tobacco etch virus protease/10 mg of eluted protein for 10 min at room temperature followed by overnight incubation at 4 °C. The digested eluate was passed over a nickel-chelating resin pre-equilibrated with HEPES.

Construction of the GAS Surface Protein Microarray—The GAS protein array was generated by spotting purified recombinant proteins (0.5 mg/ml) in four replicates on nitrocellulose-coated slides (FAST slides; Schleicher & Schuell) using the contact-printing spotter Chipwriter Pro (Bio-Rad), fitted with quill pins, resulting in spots of ~150 μm in diameter. As experimental controls, three curve replicates of biotinylated BSA and mouse IgG(s) (from 0.008 to 1 mg/ml) were spotted on the arrays. PBS buffer was spotted in at least twice the number of the protein spots and used to detect nonspecific signals caused by cross-contamination during spotting. Fewer than 5% of the PBS spots showed signal intensity higher than the background value +3 standard deviation values. Array spotting was validated by confirming the presence of all immobilized proteins using mouse antisera raised against the recombinant proteins and a Cy3-labeled α-mouse IgG secondary antibody for detection of positive signals. For protein interaction experiments, protein probes were biotinylated using the amine-reactive biotinylation reagent EZ-Link Sulfo-NHS-LC-LC-Biotin (Pierce) in a reagent:protein molar ratio of 3:1.

Nonspecific binding was minimized by preincubating arrays with a blocking solution containing 5% Top Block (Fluka-BioChemiKa) and 0.05% Tween 20 in PBS buffer (TPBS). After washing with TPBS, biotinylated proteins were diluted in 3% Top Block-TPBS and overlaid on the arrays (10–20 pmol in 100 μl) at 20 °C for 1 h. Interactions were detected by incubating the arrays with Streptavidin-Cy3 (1:100) at 20 °C for 1 h. All of the incubation steps were conducted under agitation using the HS 4800 hybridization station (TECAN). Image fluorescence signals were detected with a ScanArray 5000 scanner (Packard, Billerica, MA), and the 16-bit images were generated with ScanArray™ software at 10 μm/pixel resolution and spot fluorescence intensities were determined using ImaGene 6.0 software (Biodiscovery Inc.). Microarray data analysis was performed using in-house developed software. For each protein, the mean fluorescence intensity (MFI) of replicated spots was determined, after subtraction of the background value surrounding each spot. Signals were considered as positive when their MFI value was higher than 5,000, corresponding to the MFI of protein spots after detection with Streptavidin-Cy3 alone, plus 3 standard deviation values.

Protein Immobilization for Surface Plasmon Resonance Analysis—Experiments were performed at 25 °C with a BIACORE T100 instrument (Biacore AB, Uppsala, Sweden). All of the reagents were purchased from GE Healthcare, when not specified. The SpeI, AdcA, and Lmb proteins were immobilized on a carboxymethylated dextran-coated (CM5) sensor chip by amine coupling. Briefly, a mixture of 0.2 M 1-ethyl-3-diaminopropyl-carbodiimide and 0.05 M *N*-hydroxysuccinimide was used for sensor chip surface activation. Proteins preconcentrated in 0.01 M sodium acetate, pH 4.5, were injected at 50 μg/ml for 7 min, and then 1 M ethanolamine pH 8.5 was used to block any remaining activated groups. Approximately 2000 resonance units of immobilized material were obtained for the three proteins. In all of the experiments, an empty flow cell was used as a blank reference, and subtracted sensorgrams were used for evaluation.

Influence of Zn^{+} on Binding—Binding on immobilized proteins was investigated either in the absence or in the presence of zinc ions. 10 mM HEPES, 150 mM NaCl, 0.05% p20, pH 7.4 (HBS-N) with increasing $ZnCl_2$ (Sigma-Aldrich) concentrations, ranging from 100 nM to 50 μM, was used as running buffer. Proteins diluted in the same buffer at

[1] The abbreviations used are: GAS, group A *Streptococcus*; MFI, mean fluorescence intensity; PLA, proximity ligation assay; SPR, surface plasmon resonance.

[2] N. Norais and G. Grandi, unpublished observation.

50 and 25 μg/ml were injected for 3 min at a flow rate of 20 μl/min, and regeneration of sensor chip surface was achieved with a 30-s pulse of 500 nM NaCl and 10 mM EDTA. HBS-EP+ was used as running and dilution buffer for the same experiments without Zn^{2+}.

K_{off} Ranking—Selected proteins were diluted at 25 μg/ml in HBS-N/5 μM Zn^{2+} and then injected over the three proteins simultaneously for 3 min at a flow rate of 20 μl/min. Dissociation was followed for 400 s, and regeneration was performed as already described. Dissociation rate constants were calculated with BiaEvaluation 4.1 software.

Kinetics Characterization—The proteins SpeI, AdcA, and Lmb were further characterized for their association rate and affinity constants at equilibrium *versus* immobilized proteins. Kinetics experiments were performed by injecting an increasing concentration, from 2 nM to 1 μM, of the proteins in HBS-N/5 μM Zn^{2+} over the sensor chip surface for 3 min at a flow rate of 20 μl/min. Complexes were left to dissociate for 500 s, and regeneration was obtained with a 30-s pulse of 500 nM NaCl and 10 mM EDTA. Each protein was diluted shortly before injection to minimize potential aggregation. k_{on}, k_{off}, and K_D were calculated with the 1:1 Langmuir model using BiaEvaluation 4.1.

Confocal Immunofluorescence Microscopy—To visualize proteins on the bacterial surface, strain 3348 was grown in 5 ml of Todd Hewitt Yeast Extract (THYE) up to A_{600} = 0.4 and washed in PBS. Bacterial pellets were resuspended in 0.5 ml of a PBS, 0.025% Tween 20 solution containing sequencing grade trypsin (Promega) at a final concentration of 40 μg/ml and incubated for 30 min at 37 °C. Bacteria were then washed with PBS and reinoculated in 5 ml of fresh THYE for times from 30 min to 2 h at 37 °C. Paraformaldehyde was added to the culture medium to a final concentration of 2%. The cells were fixed for 20 min at room temperature and spotted onto POLYSINE™ slides (Menzel-Glaser). The slides were then blocked with PBS containing 10% normal goat serum and 3% BSA for 30 min and incubated with a mix of rabbit antibodies and biotinylated wheat germ agglutinin diluted in PBS with 1% BSA for 15 min at room temperature. The bacteria were then stained with goat anti-rabbit Alexa Fluor-conjugated antibodies and streptavidin (excitation at 488 and 568 nm, respectively) (Molecular Probes) for 10 min at room temperature. ProLong Gold Antifade reagent (Molecular Probes) was used to mount coverslips. The slides were analyzed with a Zeiss Observer LSM 710 confocal scanning microscope.

PLA was performed according to the manufacturer instructions (Duolink II PLA; Olink Bioscience, Uppsala, Sweden) (21–24). The assay is based on dual binding by a pair of proximity probes (antibodies with attached DNA strands) to a target protein complex, followed by the addition of oligonucleotides designed to produce a circular DNA molecule after being joined by ligation. The circular DNA molecule is then amplified by rolling circle amplification primed by one of the proximity probes, thus creating a concatemeric amplification product that remains covalently attached to the proximity probe. The rolling circle amplification product can subsequently be detected by hybridization of fluorescence-labeled oligonucleotides.

RESULTS

Microarray Design—To identify interactions between surface-exposed or secreted *S. pyogenes* proteins, we used protein microarrays carrying 83 GAS proteins. All of the GAS proteins printed on the arrays were selected using a combined bioinformatics and proteomic approach (6, 25). In addition to a signal peptide, the selected proteins carry either a lipoprotein signature, an LPXTG cell surface anchor motif, or host cell-binding domains such as RGD. Finally, some of the selected proteins have sequence similarity to known surface proteins or known virulence factors from other bacteria (Table I). All of the selected proteins belong to the *S. pyogenes* M1 strain SF370 except for one M3 (strain MGAS315), one M6 (strain MGAS10394), and two M12 (strain 2728) proteins annotated as fibronectin binding (26) and used as controls of binding conditions.

The mature form of each GAS protein was expressed in *E. coli* as a C-terminal His tag fusion protein and purified from the bacterial soluble fraction using a high throughput three-step purification system that yields proteins at 70–90% purity (19) (Fig. 1*A*). After purification, the proteins were printed on nitrocellulose-coated glass slides in quadruplicate, and protein immobilization was confirmed by incubation with mouse antisera raised against the recombinant proteins and the His tag, followed by detection with a Cy3-labeled α-mouse IgG secondary antibody and fluorescence scanning (see "Experimental Procedures").

Biotinylated BSA (BSA-Biotin) was also spotted on the array at different concentrations (from 0.008 to 1 mg/ml, four replicates) and used as a detection control. Mean fluorescence intensities of BSA-Biotin spots obtained after detection with Cy3-conjugated streptavidin were fitted best by sigmoid curves, showing a signal dynamic range of about 2 logs of fluorescence intensity values and a lower detection limit corresponding to ~0.03 ng (Fig. 1*B*). Other samples were printed on the array and used as controls for spotting and detection, including mouse IgGs and PBS buffer, which was spotted on either side of each protein spot and used to detect protein carryover during spotting. Fewer than 5% of PBS spots showed signal intensities higher than the background value.

Interactions with proteins immobilized on the array were identified by using biotinylated proteins as probes. Each purified GAS protein was biotinylated using an amine-reactive biotinylation reagent at a 3:1 molar ratio (3 mol of biotin/mole of protein) to avoid modification of all exposed lysine residues, thus hampering the accessibility of putative sites of interaction with other proteins. Ten of the biotinylated proteins were analyzed by mass spectrometry, and their biotin-linked residues were mapped. A representative example of such an analysis is given in Fig. 1*C*, which shows that for our experimental conditions Spy1007 (SpeI), which contains 21 lysine residues in its sequence, was biotinylated only at one, two, or three lysine residues per protein molecule, and biotin was linked only to Lys^{100} and/or Lys^{207} and/or Lys^{225}. Analogous results were obtained for the other proteins analyzed by mass spectrometry. In all cases, between one and three lysine residues were biotinylated, and the modification was observed to occur at a restricted number of sites.

Each biotinylated protein was used to probe the protein microarrays. Protein-protein interactions were detected by the addition of fluorophore-conjugated streptavidin, and positive spots were visualized by fluorescence scanning. In each experiment, arrays probed with labeled streptavidin only were run in parallel as negative controls, giving always negligible

TABLE I
Annotation and predicted localization of proteins used for microarrays

Protein predicted localization	Number	Annotation (SF370 NCBI)	Locus
Lipoprotein	23	Energy metabolism	*lmb; mtsA; tlpA;* SPy0163; SPy1228
		Transport and binding proteins	*fhuD; oppA; pstS;* SPy0317*;* SPy1274*;* SPy1795
		Cell envelope	*dppA;* SPy0604*;* SPy1290
		Unknown function	*inlA; malX*; *prsA*; SPy0210; SPy0252; SPy0457; SPy0778; SPy1294; SPy1390
Membrane	36	Energy metabolism	*lmb; mtsA; tlpA;* SPy0163; SPy1228
		Amino acid biosynthesis	*cysM*
		Cell envelope	*isp*; *prtS*; SPy0793; SPy0843; SPy1326
		Cell wall/membrane biogenesis	SpyM3_0104
		Cellular processes	*hlyA1*
		Central intermediary metabolism	*glmS*; SPy0380
		Energy metabolism	*guaA*; *pulA*
		Fatty acid and phospholipid metabolism	*accA*
		Protein fate	*scpA*
		Transport and binding proteins	SPy2009; SPy2033; M6_Spy0157
		Unknown function	*cbp*; *emm1*; *fabK*; *ftsZ*; *gid*; *grab*; *mf*; *pepQ*; *prgA*; SPy0128; SPy0130; SPy0838; SPy0872; SPy1054; SPy1686; SPy1874; SPy1939; gi-19224134; gi-19224141
Outside	20	Cell envelope	*isp2*; *mur1.2*
		Cellular processes	*hylA; ska*; *speC*; *speG*; *speI*; *speJ*
		Central intermediary metabolism	SPy1718
		Unknown function	*adcA*; *mf3*; *sic*; *slo*; SPy0019; SPy0925; SPy1037; SPy1491; SPy1733; SPy1813; SPy2066
Cytoplasm	2	Cell envelope	*fbp*
		Energy metabolism	*eno*
Unknown	2		SPy0652; SPy1959

fluorescence signals (Fig. 1*B*). Validation of the experimental conditions used for detecting protein-protein interactions was obtained by probing the arrays with biotinylated human fibronectin. As shown in Fig. 1*D*, the four proteins on the microarrays annotated as fibronectin-binding (supplemental Table S1) were positive for binding to human fibronectin under our experimental conditions.

Protein-Protein Interactions—On the basis of the results of the validation experiments, we arbitrarily set as a constraint for scoring a positive result as a real interaction that the MFI values be greater than 5000 (equal to the mean signal of protein spots after detection with Streptavidin-Cy3 alone, plus three standard deviation values). Overall, 146 interactions involving 71 proteins were scored as positive. A representation of the network of all of the interactions showing MFI values higher than 5000 is given in Fig. 2. The interactions include 38 networks comprising at least three interactors. Among the "nodes" involved in interactions with more than a few proteins, only seven have been annotated with an assigned function: OppA, DppA, PrsA, Mur1.2, Lmb, TlpA, and SpeI. In Gram-positive bacteria, the oligopeptide permease OppA and the dipeptide permease DppA are membrane-associated lipoproteins that belong to the ABC-transporter family responsible for the uptake of oligopeptides and dipeptides, respectively (27). Under our experimental conditions, biotinylated OppA binds seven proteins including PrsA (Fig. 2). In *B. subtilis*, PrsA is an essential lipoprotein component of the protein secretion pathway, where it functions on the *trans* side of the cytoplasmic membrane as a post-translocational folding factor (28). *B. subtilis* PrsA has been shown to exhibit peptidyl prolyl *cis*/*trans*-isomerase activity, a function essential for the stability and secretion of several exoproteins (29), and in *S. pyogenes* PrsA was found to be required for the final maturation steps of SpeB, a pluripotent cysteine protease and an important virulence factor (30). Another interesting network of interactions is that of TlpA, a chaperone of the thiol-disulfide isomerase and thioredoxins family, that binds PrsA and, at the same time, the virulence factors SpeI and Lmb. These data suggest that PrsA and TlpA may form a complex involved in the folding of several virulence factors. Similarly, the *S. pyogenes* homologue of Mur1.2, a peptidoglycan hydrolase of the FlgJ family whose activity in *Salmonella* has been shown to be required for penetration of the peptidoglycan layer by the flagellum (31), was found to interact with important virulence factors secreted into the extracellular space (HylA, Ska, Slo, and SpeI), as well as with C5A peptidase (ScpA), with a fimbrial structural subunit (M6_Spy0160) and with two F2-like fibronectin-binding proteins (SpyM3_0104 and gi-19224141) (26, 32, 33). All of these factors need to make their way through the bacterial peptidoglycan layer to reach the extracellular space where they can come into contact with their targets. Thus, it is plausible that an association with the

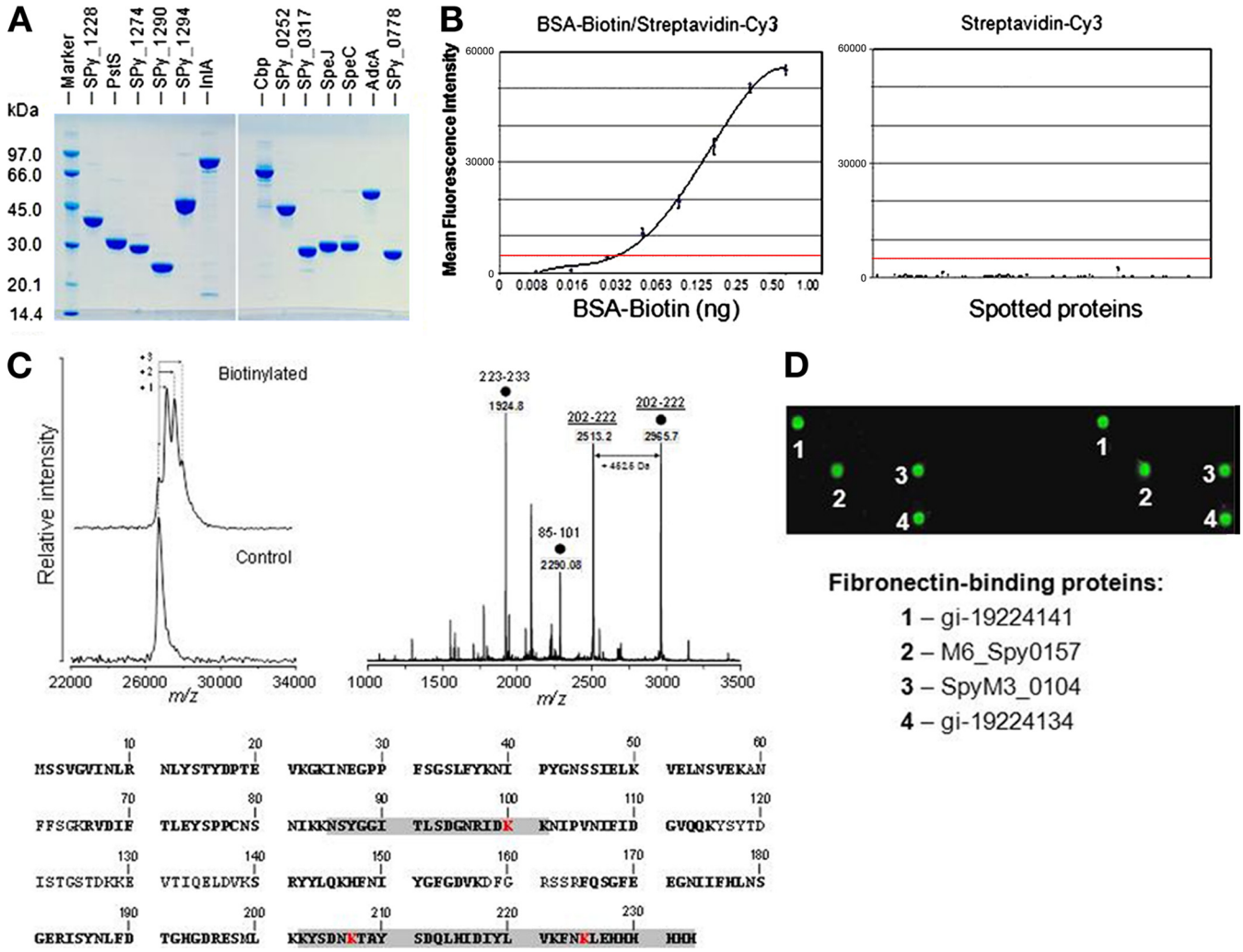

FIG. 1. **Protein analysis and microarray validation.** *A*, high throughput three-step protein purification using an AKTAxpress chromatography system yields proteins at 70–90% purity. Coomassie-stained SDS-PAGE gel of proteins was purified by AKTAxpress chromatography and used for microarray experiments. *B*, graphic representation of the BSA-Biotin control curve. *Dots* correspond to the different BSA-Biotin concentrations indicated on the *x* axis, whereas the *continuous line* corresponds to the interpolated resulting curve. MFI values are reported on the *y axis*. The graphic representation of the distribution of MFI values measured after incubation with Cy3-labeled streptavidin alone (negative control) is shown in the *right panel*. *C*, analysis of the biotinylated recombinant protein Spy1007 by mass spectrometry. MALDI-TOF MS spectra of the modified/unmodified protein are reported in the *left panel*. Spectra of unmodified (*lower spectrum*) and modified recombinant Spy1007 (*upper spectrum*) were acquired in linear mode. The singly charged monomer $[MH]^+$ (1) observed from the unmodified protein is in agreement with the theoretical mass of the protein (26.8 kDa). After the biotinylation reaction, the protein was observed with singly charged monomers $[MH]^+$ in agreement with the masses of the unmodified protein and with the mass of the protein increased by one, two, or three biotinylation adducts. The mass difference between the $[MH]^+$ species is in agreement with the biotinylation adduct (669.75 Da). The peptide mass fingerprint of the biotinylated protein is reported in the *right panel*. The protein was digested with the endoprotease LysC, and the generated peptides were analyzed by MALDI-TOF MS in reflectron mode. The biotinylated peptides are assigned with a *dot*, the mass shift caused by the biotinylation adduct is indicated with an *arrow*. The three biotinylated lysines identified are indicated in *red* in the protein sequence reported in the *lower panel*. The identified peptide sequences are assigned in *bold type*. *D*, validation of protein-protein interaction experiments. A microarray was probed with biotinylated human fibronectin, and interactions were visualized by incubating the array with Cy3-labeled streptavidin and fluorescence scanning. After data processing, four proteins had signals above background.

Mur1.2 homologue may facilitate their becoming more readily exposed to the extracellular environment.

Finally, SpeI is one of the potent toxins secreted by GAS that belong to the family of superantigens, proteins that share a high degree of structural similarity (34) and whose primary function is to induce antigen-independent T cell activation. SpeI showed a surprisingly complex network of interactions, involving ~70% of all the proteins analyzed in this work. The "sticky" property of SpeI can be explained considering the unique capacity of superantigens to interact with different MHC molecules and T cell receptors. However, SpeC, SpeG, and SpeJ, the other three superantigens secreted by the

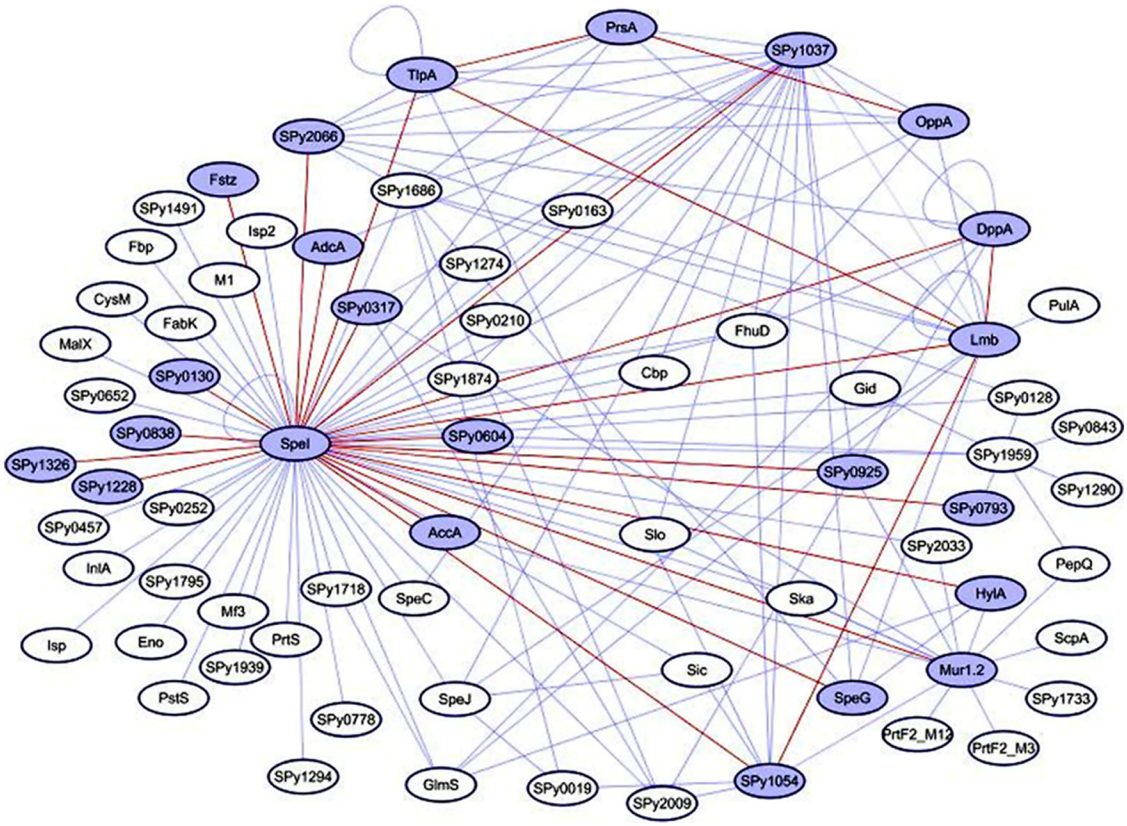

FIG. 2. **Interactions between *S. pyogenes* surface-exposed or secreted proteins.** The networks of interactions were visualized using Cytoscape (52). The nodes represent proteins, whereas each edge represents an interaction between the two proteins. Nodes of reciprocal interactions are indicated by *blue-filled circles* joined by *red lines*.

SF370 strain and included in our protein arrays, showed a very restricted binding capacity involving three proteins only. All three bound SpeI and the hypothetical protein Spy1037, whereas SpeG and SpeJ, but not SpeC, were also capable of recognizing Lmb.

Validation of Protein Interactions—The 146 identified interactions are expected to include both low and high affinity bindings. Protein array is a semi-quantitative platform that cannot precisely discriminate one type of interaction from the other. However, the chip analysis provides two sets of data that can be used to tentatively rank protein complexes on the basis of their affinity of interaction. First, because the experimental design is such that each protein is tested twice for its capacity to bind to a possible partner (in one case the protein is fixed on the nitrocellulose surface and the partner is in solution, and in the other case, the protein is in solution and the partner immobilized), interactions detected for both situations ("reciprocal" interactions) are expected to generate relatively stable complexes. Overall, 25 of the 146 two-protein complexes were detected irrespective of which of the proteins were in solution or immobilized. The 23 proteins participating in the 25 reciprocal interactions included SpeI, which was involved in most of the interactions, 11 proteins classified as hypothetical or with unknown function, and 12 well characterized proteins. Altogether, they formed a total of six networks/complexes (Fig. 3). Second, as we have recently shown in a study aimed at identifying new host-pathogen interactions (35), MFI appears to directly correlate with affinity constants of protein-protein interaction. In this context, it is noteworthy that reciprocal interactions showed significantly higher MFI values compared with the unilateral interactions (MFI: 15118.93 *versus* 7973.24) (supplemental Fig. S1).

Several of the SpeI interactors belong to the molecular chaperone or protein folding catalyst families and, presumably, are involved in the secretion and folding of the superantigen. SpeI contains a single cysteine residue at position 80 involved in intermolecular disulfide bond formation and has been shown to exist in monomer-dimer equilibrium (36). In fact, we found interaction of SpeI with itself and, also, with the protein disulfide reductase SPy1558/TlpA and with SPy0925, a putative oxidoreductase. Moreover, one of the SpeI interactors was SpeG, suggesting that these two superantigens may form heterodimers as well as homodimers. In addition, the substrate binding subunits of two transition metal transporters (AdcA and Lmb) were found to interact with SpeI. This finding is particularly important because SpeI has been shown to bind MHC-II molecules in a zinc-dependent manner (34), and AdcA is an orthologue of the high affinity zinc uptake

SPy number	Protein name	Annotation
SPy0293	OppA	Oligopeptidepermease
SPy0130		Hypothetical protein
SPy0212	SpeG	Exotoxin G precursor
SPy0317		Hypothetical protein
SPy0604		Hypothetical protein
SPy0714	AdcA	Zinc-binding protein adcA/ putative adhesion protein
SPy0793		Hypothetical protein
SPy0838		Hypothetical protein
SPy0857	Mur1.2	Putative peptidoglycan hydrolase
SPy0925		Putative oxidoreductase
SPy1007	SpeI	Streptococcal exotoxin I
SPy1032	HylA	Extracellular hyaluronate lyase
SPy1037		Hypothetical protein
SPy1054		Putative collagen-like protein
SPy1228		Putative lipoprotein
SPy1326		Outer surface protein
SPy1520	FtsZ	Cell division protein
SPy1558	TlpA	Thioredoxin[a]
SPy1743	AccA	Acetyl-CoA carboxylase alpha subunit
SPy2000	DppA	Dipeptide-binding protein
SPy2007	Lmb	Putative laminin adhesion
SPy2037	PrsA	Foldase protein (peptidylprolyl isomerase)
SPy2066		Putative dipeptidase

[a] (53)

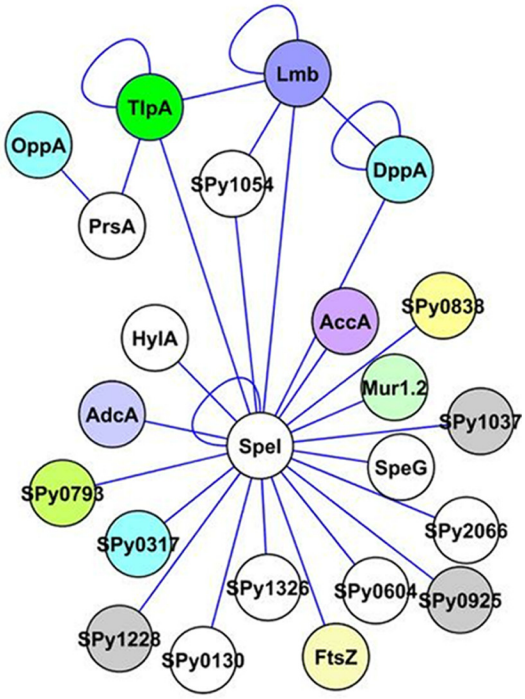

FIG. 3. **Networks representing all the reciprocal interactions identified.** The *table* on the *left* reports the NCBI annotation for each protein involved in a reciprocal interaction.

system protein ZnuA, whereas Lmb belongs to the general transition metal transporter TroA family that binds iron, Mn^{2+}, and Zn^{2+} with similar affinities (37).

Fourteen of the protein-protein interactions identified with microarrays were analyzed using surface plasmon resonance (SPR). Twelve of the interactions belong to the group of reciprocal interactions (including two proteins forming homodimers), and two were unilateral interactions. To avoid interference of the His tags present in the proteins purified for the microarrays, for the SPR experiments the proteins were re-expressed using an N-terminal translational fusion of the His_6 purification tag followed by a tobacco etch virus protease cleavage site for subsequent TAG removal after the first affinity purification step. Thus, all of the proteins chosen for SPR analysis were purified as tag-less forms. SPR experiments were performed at 25 °C with a BIACORE T100 instrument. Ligand proteins were immobilized on a carboxymethylated dextran-coated (CM5) sensor chip by amine coupling. Binding to immobilized proteins was investigated either in the absence or presence of zinc ions. Analyte proteins were diluted in running buffer (10 mM HEPES, 150 mM NaCl, 0.05% p20, pH 7.4, 5 μM $ZnCl_2$) and injected for 3 min at a flow rate of 20 μl/min. As shown in Table II, all of the interactions identified using protein microarrays were also detected by SPR with dissociation rates (k_{off}) typical of stable interactions, ranging from 1.4×10^{-4} to 3.9×10^{-3} s^{-1}.

TABLE II
SPR analysis of dissociation kinetics (k_{off}) between interactors

In solution	Immobilized	k_{off}(s^{-1} 10^{-4})	k_{off}(s^{-1} 10^{-4})
Reciprocal			
SpeG	SpeI	8.2	
AdcA	SpeI	18.0	8.1
SPy_1054	SpeI	2.8	
SPy_1054	Lmb	2.0	
DppA	SpeI	4.5	
DppA	Lmb	1.4	
Lmb	SpeI	35.0	7.4
SPy_2066	SpeI	3.4	
SPy_1326	SpeI	2.7	
SPy_0925	SpeI	2.0	
Unilateral			
SpeG	Lmb	8.7	
SPy_2066	Lmb	3.2	
SpeI	SpeI	10.0	
Lmb	Lmb	38.7	

A more detailed SPR analysis was carried out for the interactions of SpeI with the two zinc transporters. Because it is known that Zn^{2+} is required for SpeI activity (34), similar to the previous experiments involving SpeI, SPR analysis was carried out in the presence and absence of 5 μM $ZnCl_2$. The results shown in Fig. 4 clearly demonstrate that the superantigen interacts strongly with both transporters in the presence of 5 μM Zn^{2+}, and both display higher association constants with SpeI

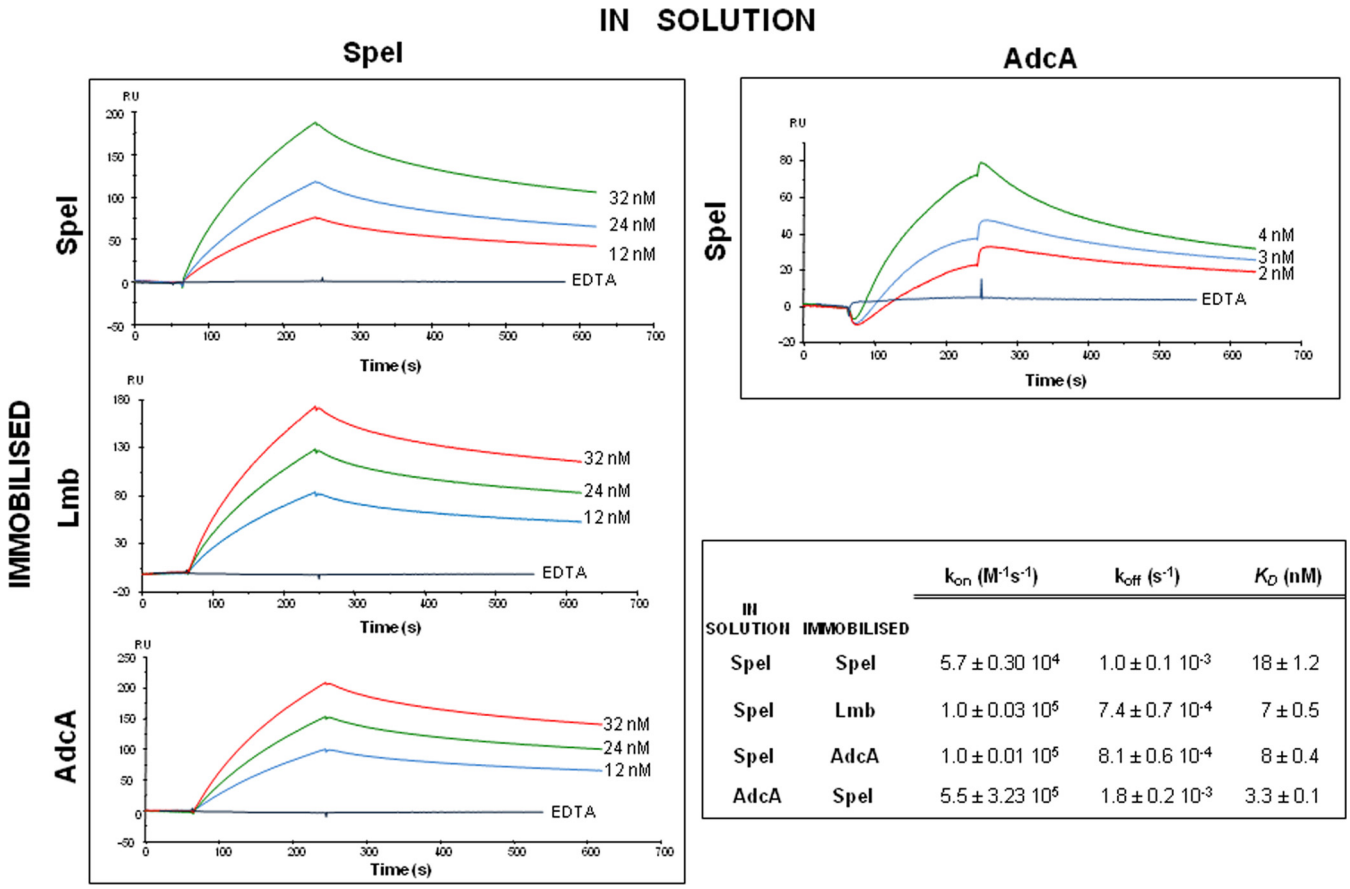

IN SOLUTION	IMMOBILISED	k_{on} ($M^{-1}s^{-1}$)	k_{off} (s^{-1})	K_D (nM)
SpeI	SpeI	$5.7 \pm 0.30\ 10^{4}$	$1.0 \pm 0.1\ 10^{-3}$	18 ± 1.2
SpeI	Lmb	$1.0 \pm 0.03\ 10^{5}$	$7.4 \pm 0.7\ 10^{-4}$	7 ± 0.5
SpeI	AdcA	$1.0 \pm 0.01\ 10^{5}$	$8.1 \pm 0.6\ 10^{-4}$	8 ± 0.4
AdcA	SpeI	$5.5 \pm 3.23\ 10^{5}$	$1.8 \pm 0.2\ 10^{-3}$	3.3 ± 0.1

FIG. 4. **SPR analysis of SpeI interactions with AdcA and Lmb.** The SpeI, AdcA, and Lmb proteins purified in a tag-less form were immobilized on a carboxymethylated dextran-coated (CM5) sensor chip by amine coupling. Kinetics experiments were performed by injecting an increasing concentration of analyte protein in HBS-N in the presence of 5 μM Zn^{2+} over the sensor chip surface for 3 min at a flow rate of 20 μl/min. Complexes were left to dissociate for 500 s. The curves corresponding to three intermediate concentrations of analyte protein are shown. The presence of 10 mM EDTA abrogated binding for all samples. k_{on}, k_{off}, and K_D were calculated with the 1:1 Langmuir model using BiaEvaluation 4.1.

than SpeI with itself. AdcA binds the superantigen with the highest affinity (K_D = 3.3 nM) when in solution, whereas similar affinities were found for both AdcA and Lmb with SpeI in solution (Fig. 4). Finally, the affinity constant of SpeI dimer formation for our experimental conditions was K_D = 18 nM, the same value reported for Ras-GTP binding of RafRBD (38), the benchmark of protein-protein interactions. All of these interactions were abrogated by the addition of 10 mM EDTA (Fig. 4).

Localization of Interactors on the Bacterial Surface—To verify whether proteins interacting *in vitro* on the protein chip are found *in vivo* at the same bacterial district, the localization of a number of SpeI interactors was analyzed by confocal microscopy. Two approaches were used: (*a*) synchronizing bacteria with trypsin and staining proteins as soon as they are re-exported and (*b*) highlighting the close proximity of the interactors by PLA technology.

Cells were treated with trypsin to remove proteins exposed on the bacterial surface and then allowed to resume growth in rich medium before fixation and staining with specific antibodies. The export of several interactors (AdcA, TlpA, Lmb, Mur1.2, FtsZ, and SpeG) was monitored by visualizing their reappearance on the surface at different time points. M protein, one of the best characterized surface proteins of *S. pyogenes*, was used as a control. Representative results of this analysis are given in Fig. 5. Immediately after trypsin treatment (*top panel* at *time 0* in Fig. 5) no M protein could be detected, whereas 30 min after growth recovery protein M was clearly visible at foci localized at regions coincident with the cell septum, where it is known to anchor to newly synthesized cell wall (39–41). Ultimately, 60 min after the removal of trypsin, M protein became distributed over the entire cell surface (*top panel* at time *60 min* in Fig. 5). Staining with antibodies specific for SpeI, TlpA, AdcA, or the other interactors tested at 30 min after the removal of trypsin showed a distribution of these proteins to foci at septal regions, as observed for M protein at the same time point. However, at 60 min they were still localized at the septum, where they were seen to remain until the end of the observation time (120 min). Unlike M protein, which, after being covalently linked to peptidoglycan at the septum, is distributed over the whole cell

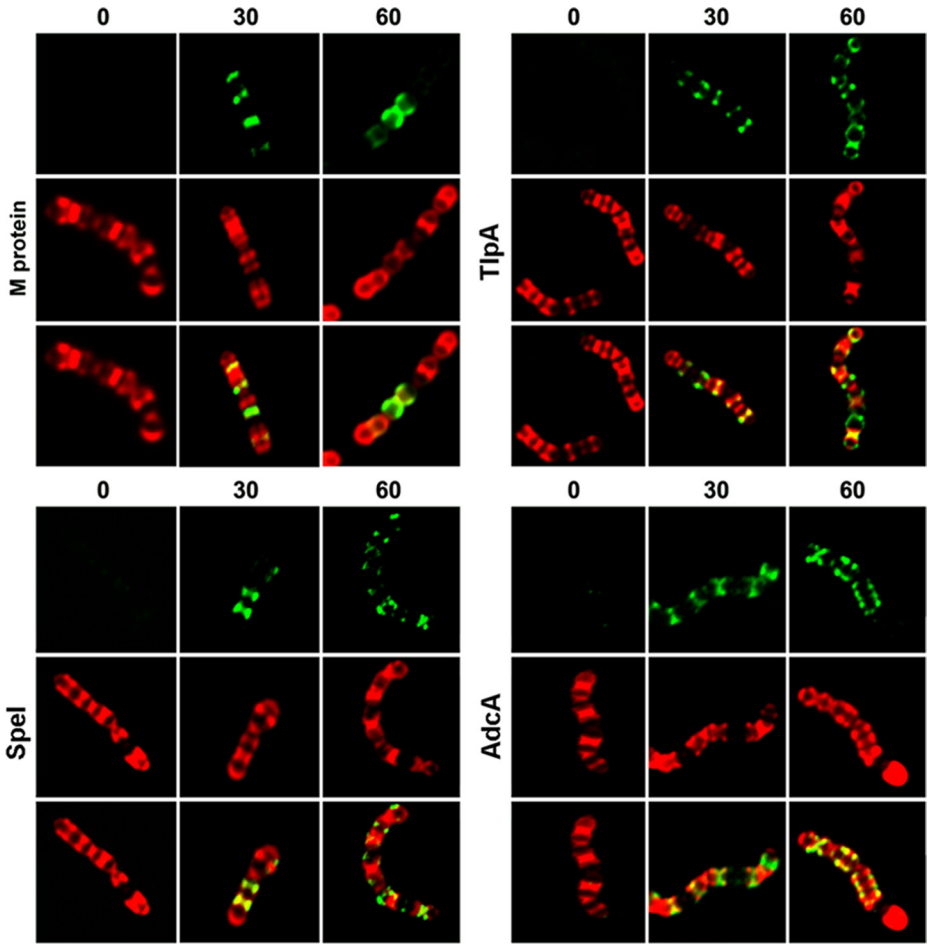

FIG. 5. **SpeI and its interactors localize to similar districts of the bacterial surface.** *S. pyogenes* strain 3348 cells were treated with trypsin, washed, and inoculated in medium without trypsin for 0, 30, or 60 min before fixation (see "Experimental Procedures"). The cells were stained for M protein, SpeI, TlpA, or AdcA using goat anti-rabbit antibodies (*green*) and for cell wall peptidoglycan with biotinylated wheat germ agglutinin (*red*). For each sample, merging of the two images is shown in the *bottom panel*.

surface during progression of cell wall synthesis, these proteins after translocation become associated with the cell membrane and remain located at specific foci. Similar results were also obtained for OppA, Lmb, Mur1.2, HtrA, and SpeG (data not shown).

The close proximity of interactome proteins *in vivo* was confirmed by use of the *in situ* proximity ligation assay (*in situ* PLA) (42). Briefly, this assay allows the detection of protein proximity localization by using antibodies attached to oligonucleotide probes that allow the detection of two specific antigens only when they are in a narrow spatial range (≤40 nm). For the detection of interactors situated in close proximity at specific bacterial districts, we used pairs of antibody-conjugated oligonucleotides that were joined by ligation only if they have been brought in proximity by the interacting antigens. The DNA ligation products were then amplified by *in situ* PCR, and a fluorescent complementary DNA probe was used for detection of the PCR product. We tested the interactors shown in Fig. 6 and found that they localize at the bacterial septum. In particular, we used SpeI as the bait protein and AdcA (Fig. 6*B*), TlpA (Fig. 6*C*), and OppA (Fig. 6*D*) for proximity localization. As shown in Fig. 6, the three proteins were all close enough to SpeI to be revealed by the PLA assay. As a negative control, we used a single primary antibody, and detection of any signal was revealed by the respective secondary antibodies (+ and −), or we used secondary antibodies without preincubation with specific primary antibodies. No signal was observed under these conditions (Fig. 6*A*). These data support our hypothesis for a close association of such interactors, as indicated by the *in vitro* microarray results.

Moreover, to prove that the localization of interactome proteins to the cell septum is driven by specific interaction of the protein with elements present at this district, bacteria were grown until they reached the exponential phase, and then recombinant forms of SpeI, SpeC, and GraB were added ectopically to the bacterial cultures. These were chosen because they represent proteins known from the microarray analysis to have no (SpeC and GraB) or many (SpeI) interactors. Also, we used strain MGAS5005 (43) because it lacks genes coding for SpeC and SpeI and does not express GraB during the exponential phase of growth. This allowed us to add recombinant exogenous forms of such antigens without the interference of endogenously expressed SpeC, SpeI, and GraB. As expected, SpeI redirected to the septum after 10 min of incubation with bacteria (supplemental Fig. S2*A*). When

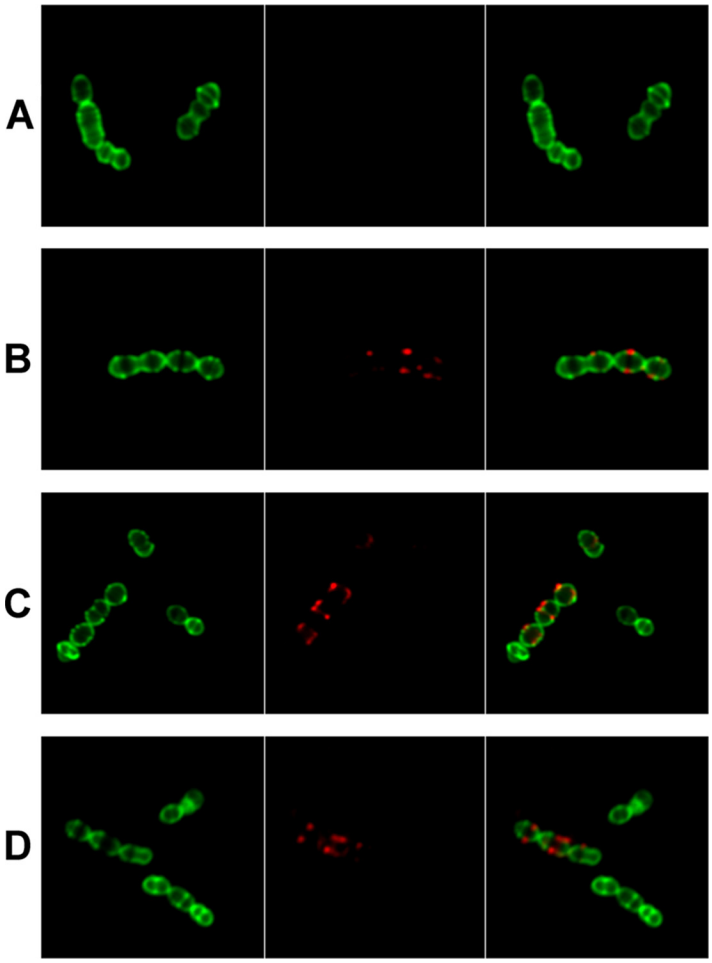

FIG. 6. **SpeI and its interactors localize in close proximity at the bacterial septum.** PLA staining of complexes was performed as described under "Experimental Procedures." *A*, control bacteria; *B*, SpeI-AdcA; *C*, SpeI-TlpA; *D*, SpeI-OppA. For each sample, merging of the two images is shown in the *right panel*.

we added recombinant exogenous SpeC (supplemental Fig. S2*B*) and GraB (supplemental Fig. S2*C*), known to have no interactors from the microarray analysis, we did not observe any association of these proteins with the bacterial surface. These data confirm the specificity of the interaction of SpeI with its cellular target and allow us to conclude that SpeI seems to be exported to the same districts of the bacterial surface as TlpA, AdcA, Lmb, Mur1.2, FtsZ, and SpeG. In particular, double staining of the same cells using anti-SpeI and anti-AdcA antibodies demonstrated that the two proteins localize to the same foci (data not shown).

DISCUSSION

As the tools for determining the composition of the cell surface of bacteria develop into increasingly more advanced approaches, it is now important to pursue methods that allow the definition of the architecture of the bacterial cell surface. Indeed, although high resolution visualization of viruses and subcellular organelles has become technically feasible, and this has enormously improved the knowledge of their biology and functions, our understanding of bacterial cell surface structure in tridimensional space is still very rudimentary. In an attempt to provide a general approach to better define the topological organization of bacterial cells, herein we have taken advantage of the availability of a quite detailed map of surface and secreted proteins of *S. pyogenes* to address the question regarding whether such proteins are involved in sufficiently stable interactions that might enable us to explore novel biological mechanisms and functions.

Eighty-three recombinant proteins were analyzed for their possible interactions using protein microarray technology. Of this group of proteins, 36 carry membrane spanning domains and, among these, 15 have an LPXTG cell surface anchor motif, and three have the RGD host cell binding domain. Of the remaining 47 proteins, 43 contain a signal peptide sequence and are exported to the outside, 23 of which become attached to the membrane as lipoproteins.

Our microarray analysis revealed that this selected group of proteins gives rise, at least *in vitro*, to 146 different binary protein-protein interactions, suggesting that the bacterial surface is quite a dynamic environment, with complexes being formed among surface proteins and between surface and secreted proteins. On the basis of the MFI values obtained, which in some cases approach the saturation threshold, a non-negligible number of these interactions appear to be sufficiently strong, with affinity constants $\geq 10^7$ M^{-1}. Such

values have, in a few cases, been experimentally calculated using SPR and, for most interactions, have been extrapolated on the basis of our recent work on another protein-protein interaction study (35), in which a direct correlation between MFI and K_D was found.

Our analysis is designed to test each protein-protein interaction twice, with each protein partner being used both in the solid (immobilized on the chip) and liquid phases. Therefore, those interactions that appear to be "reciprocal" (binding between two proteins occurs irrespective of which of the two partners was immobilized on the chip or in solution) are expected to be particularly strong. Twenty-five of 146 interactions were identified as reciprocal (Fig. 3), and in fact, their average MFI values are significantly higher than the MFI values of nonreciprocal interactions. We have classified reciprocal interactions as "first priority" and will be the first to be the object of our future functional and structural studies.

A legitimate question is why most (~82%) of the interactions identified here are unilateral. Although we cannot exclude that some of them represent false-positive signals, considering the stringency of our experimental conditions, we believe that this is instead largely due to the fact that protein absorption on a solid surface can result in conformational changes sufficiently pronounced to prevent proper docking of the partner protein.

Protein interactions can generate complexes that are either stable or short-lived, as is the case for enzyme-substrate interactions. It is expected that many interactions occurring at the membrane/surface level are transient, and an interesting high throughput method to specifically single out transient interactions has been recently developed (44). We have not investigated yet the nature of the interactions found in the present study. This would require a systematic investigation of the kinetic constants (k_{on} and k_{off}) of each interaction and stability studies of protein complexes. Preliminary data using gel filtration chromatography indicate that at least some of the reciprocal interactions do not form stable complexes, suggesting that our approach is also suitable for detecting transient interactions.

The data generated in this study pave the way for new investigations aimed at understanding the biological significance of the newly identified protein-protein interactions. Although these studies are in progress, inspection of the predicted and/or experimentally demonstrated roles of the proteins involved in the interactions can prompt interesting questions that deserve urgent confirmatory experimental analysis. Two examples are particularly attractive.

Translocation of proteins across the cellular membrane in *S. pyogenes* has been reported to occur at a unique site, the ExPortal, located adjacent to the area where the septum will form (45). The existence of a single route through which proteins destined to the outside are translocated implies that the extracellular factors involved in folding of secreted proteins are also clustered in the region surrounding the ExPortal (reviewed in Ref. 46). So far, HtrA (Spy2216), a protease with

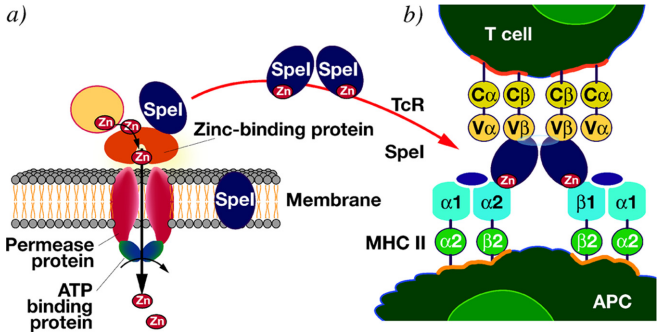

FIG. 7. **Model of the acquisition of zinc ions by SpeI.** a) Cartoon showing how interaction of SpeI with the substrate binding subunit of the Zn^{2+} transporter could occur at the site of SpeI export. b) Acquisition of Zn^{2+} ions by SpeI would subsequently result in SpeI dimer formation and binding to MHC II and TcR (36).

a chaperone function (47), is the only protein that has been unequivocally shown to belong to the ExPortal complex. Our interactome analysis revealed that other proteins involved in protein folding and transport mechanisms, including OppA, DppA, PrsA, and TlpA form complexes, and some of them also interact with HtrA (not shown). In view of our confocal microscopy analysis, which indicates that these proteins all localize at the cell septum, it is plausible that at least some of them might be part of the ExPortal complex.

The second interesting example is the identification of the interaction between SpeI and the substrate binding subunit of two transition metal transporters with different metal specificities: AdcA and Lmb. In particular, AdcA is a high affinity Zn^{2+} transporter, whereas Lmb belongs to the general transition metal transporter TroA family, which binds iron, Mn^{2+}, and Zn^{2+} with similar affinities (37, 48). Transition metals in mammalian body fluids are sequestered by carrier proteins and have very low bioavailability (49, 50). For this reason, acquisition of transition metals is a crucial task for a bacterial pathogen during infection, because iron, Mn^{2+}, and Zn^{2+} are essential for the correct structure and catalytic function of numerous proteins (51). The observation that the SpeI superantigen, which requires Zn^{2+} for binding to MHC-II molecules (34), shows a high affinity interaction with both transporters suggests that, in addition to their known role in survival in the host environment, they are also essential for pathogenicity. This finding opens a new perspective on the current understanding of how superantigens are modified by the bacterial cell to become major players in causing disease. A model of how SpeI may acquire zinc ions through the interaction with the substrate binding subunit of the Zn^{2+} transporter is presented in Fig. 7. In conclusion, a better definition of the topology of surface protein complexes ultimately would lead to a deeper knowledge of the mechanisms underlying invasion, colonization and, in general, pathogenesis.

* The costs of publication of this article were defrayed in part by the payment of page charges. This article must therefore be hereby

marked "*advertisement*" in accordance with 18 U.S.C. Section 1734 solely to indicate this fact.

[S] This article contains supplemental material.

§ Present address: Externautics, S.p.A., 53100 Siena, Italy.

‖ Present address: Istituto Nazionale Genetica Molecolare, 20122 Milan, Italy.

** To whom correspondence should be addressed: Novartis Vaccines, Via Fiorentina 1, 53100 Siena, Italy. Tel.: 39-0577-243506; Fax: 39-0577-278514; E-mail: guido.grandi@novartis.com.

REFERENCES

1. Nakai, K. (2000) Protein sorting signals and prediction of subcellular localization. *Adv. Protein Chem.* **54,** 277–344
2. Pizza, M., Scarlato, V., Masignani, V., Giuliani, M. M., Aricò, B., Comanducci, M., Jennings, G. T., Baldi, L., Bartolini, E., Capecchi, B., Galeotti, C. L., Luzzi, E., Manetti, R., Marchetti, E., Mora, M., Nuti, S., Ratti, G., Santini, L., Savino, S., Scarselli, M., Storni, E., Zuo, P., Broeker, M., Hundt, E., Knapp, B., Blair, E., Mason, T., Tettelin, H., Hood, D. W., Jeffries, A. C., Saunders, N. J., Granoff, D. M., Venter, J. C., Moxon, E. R., Grandi, G., and Rappuoli, R. (2000) Identification of vaccine candidates against serogroup B meningococcus by whole-genome sequencing. *Science* **287,** 1816–1820
3. Doytchinova, I. A., Taylor, P., and Flower, D. R. (2003) Proteomics in vaccinology and immunobiology: An informatics perspective of the immunone. *J. Biomed. Biotechnol.* **2003,** 267–290
4. Maione, D., Margarit, I., Rinaudo, C. D., Masignani, V., Mora, M., Scarselli, M., Tettelin, H., Brettoni, C., Iacobini, E. T., Rosini, R., D'Agostino, N., Miorin, L., Buccato, S., Mariani, M., Galli, G., Nogarotto, R., Nardi Dei, V., Vegni, F., Fraser, C., Mancuso, G., Teti, G., Madoff, L. C., Paoletti, L. C., Rappuoli, R., Kasper, D. L., Telford, J. L., and Grandi, G. (2005) Identification of a universal Group B *Streptococcus* vaccine by multiple genome screen. *Science* **309,** 148–150
5. Otto, A., Bernhardt, J., Meyer, H., Schaffer, M., Herbst, F. A., Siebourg, J., Mäder, U., Lalk, M., Hecker, M., and Becher, D. (2010) Systems-wide temporal proteomic profiling in glucose-starved *Bacillus subtilis*. *Nat. Commun.* **1,** 137
6. Rodríguez-Ortega, M. J., Norais, N., Bensi, G., Liberatori, S., Capo, S., Mora, M., Scarselli, M., Doro, F., Ferrari, G., Garaguso, I., Maggi, T., Neumann, A., Covre, A., Telford, J. L., and Grandi, G. (2006) Characterization and identification of vaccine candidate proteins through analysis of the group A *Streptococcus* surface proteome. *Nat. Biotechnol.* **24,** 191–197
7. Severin, A., Nickbarg, E., Wooters, J., Quazi, S. A., Matsuka, Y. V., Murphy, E., Moutsatsos, I. K., Zagursky, R. J., and Olmsted, S. B. (2007) Proteomic analysis and identification of *Streptococcus pyogenes* surface-associated proteins. *J. Bacteriol.* **189,** 1514–1522
8. Doro, F., Liberatori, S., Rodríguez-Ortega, M. J., Rinaudo, C. D., Rosini, R., Mora, M., Scarselli, M., Altindis, E., D'Aurizio, R., Stella, M., Margarit, I., Maione, D., Telford, J. L., Norais, N., and Grandi, G. (2009) Surfome analysis as a fast track to vaccine discovery: Identification of a novel protective antigen for Group B *Streptococcus* hypervirulent strain COH1. *Mol. Cell. Proteomics* **8,** 1728–1737
9. Dreisbach, A., van der Kooi-Pol, M. M., Otto, A., Gronau, K., Bonarius, H. P., Westra, H., Groen, H., Becher, D., Hecker, M., and van Dijl, J. M. (2011) Surface shaving as a versatile tool to profile global interactions between human serum proteins and the *Staphylococcus aureus* cell surface. *Proteomics* **11,** 2921–2930
10. Ferrari, G., Garaguso, I., Adu-Bobie, J., Doro, F., Taddei, A. R., Biolchi, A., Brunelli, B., Giuliani, M. M., Pizza, M., Norais, N., and Grandi, G. (2006) Outer membrane vesicles from group B *Neisseria meningitidis* delta gna33 mutant: Proteomic and immunological comparison with detergent-derived outer membrane vesicles. *Proteomics* **6,** 1856–1866
11. Berlanda Scorza, F., Doro, F., Rodríguez-Ortega, M. J., Stella, M., Liberatori, S., Taddei, A. R., Serino, L., Gomes Moriel, D., Nesta, B., Fontana, M. R., Spagnuolo, A., Pizza, M., Norais, N., and Grandi, G. (2008) Proteomics characterization of outer membrane vesicles from the extraintestinal pathogenic *Escherichia coli* DeltatolR IHE3034 mutant. *Mol. Cell. Proteomics* **7,** 473–485
12. Shoemaker, B. A., and Panchenko, A. R. (2007) Deciphering protein-protein interactions: Part I. Experimental techniques and databases. *PLoS Comput. Biol.* **3,** e42
13. Ito, T., Chiba, T., Ozawa, R., Yoshida, M., Hattori, M., and Sakaki, Y. (2001) A comprehensive two-hybrid analysis to explore the yeast protein interactome. *Proc. Natl. Acad. Sci. U.S.A.* **98,** 4569–4574
14. Uetz, P., Giot, L., Cagney, G., Mansfield, T. A., Judson, R. S., Knight, J. R., Lockshon, D., Narayan, V., Srinivasan, M., Pochart, P., Qureshi-Emili, A., Li, Y., Godwin, B., Conover, D., Kalbfleisch, T., Vijayadamodar, G., Yang, M., Johnston, M., Fields, S., and Rothberg, J. M. (2000) A comprehensive analysis of protein-protein interactions in *Saccharomyces cerevisiae*. *Nature* **403,** 623–627
15. Ho, Y., Gruhler, A., Heilbut, A., Bader, G. D., Moore, L., Adams, S. L., Millar, A., Taylor, P., Bennett, K., Boutilier, K., Yang, L., Wolting, C., Donaldson, I., Schandorff, S., Shewnarane, J., Vo, M., Taggart, J., Goudreault, M., Muskat, B., Alfarano, C., Dewar, D., Lin, Z., Michalickova, K., Willems, A. R., Sassi, H., Nielsen, P. A., Rasmussen, K. J., Andersen, J. R., Johansen, L. E., Hansen, L. H., Jespersen, H., Podtelejnikov, A., Nielsen, E., Crawford, J., Poulsen, V., Sørensen, B. D., Matthiesen, J., Hendrickson, R. C., Gleeson, F., Pawson, T., Moran, M. F., Durocher, D., Mann, M., Hogue, C. W., Figeys, D., and Tyers, M. (2002) Systematic identification of protein complexes in *Saccharomyces cerevisiae* by mass spectrometry. *Nature* **415,** 180–183
16. Gavin, A. C., Bösche, M., Krause, R., Grandi, P., Marzioch, M., Bauer, A., Schultz, J., Rick, J. M., Michon, A. M., Cruciat, C. M., Remor, M., Höfert, C., Schelder, M., Brajenovic, M., Ruffner, H., Merino, A., Klein, K., Hudak, M., Dickson, D., Rudi, T., Gnau, V., Bauch, A., Bastuck, S., Huhse, B., Leutwein, C., Heurtier, M. A., Copley, R. R., Edelmann, A., Querfurth, E., Rybin, V., Drewes, G., Raida, M., Bouwmeester, T., Bork, P., Seraphin, B., Kuster, B., Neubauer, G., and Superti-Furga, G. (2002) Functional organization of the yeast proteome by systematic analysis of protein complexes. *Nature* **415,** 141–147
17. Zhu, H., and Snyder, M. (2003) Protein chip technology. *Curr. Opin. Chem. Biol.* **7,** 55–63
18. Hesselberth, J. R., Miller, J. P., Golob, A., Stajich, J. E., Michaud, G. A., and Fields, S. (2006) Comparative analysis of *Saccharomyces cerevisiae* WW domains and their interacting proteins. *Genome Biol.* **7,** R30
19. Bhikhabhai, R., Sjöberg, A., Hedkvist, L., Galin, M., Liljedahl, P., Frigård, T., Pettersson, N., Nilsson, M., Sigrell-Simon, J. A., and Markeland-Johansson, C. (2005) Production of milligram quantities of affinity tagged-proteins using automated multistep chromatographic purification. *J. Chromatogr A* **1080,** 83–92
20. Klock, H. E., Koesema, E. J., Knuth, M. W., and Lesley, S. A. (2008) Combining the polymerase incomplete primer extension method for cloning and mutagenesis with microscreening to accelerate structural genomics efforts. *Proteins* **71,** 982–994
21. Fredriksson, S., Gullberg, M., Jarvius, J., Olsson, C., Pietras, K., Gústafsdóttir, S. M., Ostman, A., and Landegren, U. (2002) Protein detection using proximity-dependent DNA ligation assays. *Nat. Biotechnol.* **20,** 473–477
22. Gullberg, M., Gústafsdóttir, S. M., Schallmeiner, E., Jarvius, J., Bjarnegård, M., Betsholtz, C., Landegren, U., and Fredriksson, S. (2004) Cytokine detection by antibody-based proximity ligation. *Proc. Natl. Acad. Sci. U.S.A.* **101,** 8420–8424
23. Söderberg, O., Gullberg, M., Jarvius, M., Ridderstråle, K., Leuchowius, K. J., Jarvius, J., Wester, K., Hydbring, P., Bahram, F., Larsson, L. G., and Landegren, U. (2006) Direct observation of individual endogenous protein complexes in situ by proximity ligation. *Nat. Methods* **3,** 995–1000
24. Jarvius, M., Paulsson, J., Weibrecht, I., Leuchowius, K. J., Andersson, A. C., Wählby, C., Gullberg, M., Botling, J., Sjöblom, T., Markova, B., Ostman, A., Landegren, U., and Söderberg, O. (2007) *In situ* detection of phosphorylated platelet-derived growth factor receptor beta using a generalized proximity ligation method. *Mol. Cell. Proteomics* **6,** 1500–1509
25. Mora, M., Bensi, G., Capo, S., Falugi, F., Zingaretti, C., Manetti, A. G., Maggi, T., Taddei, A. R., Grandi, G., and Telford, J. L. (2005) Group A *Streptococcus* produce pilus-like structures containing protective antigens and Lancefield T antigens. *Proc. Natl. Acad. Sci. U.S.A.* **102,** 15641–15646
26. Bessen, D. E., and Kalia, A. (2002) Genomic localization of a T serotype locus to a recombinatorial zone encoding extracellular matrix-binding proteins in *Streptococcus pyogenes*. *Infect. Immun.* **70,** 1159–1167

27. Podbielski, A., and Leonard, B. A. (1998) The group A streptococcal dipeptide permease (Dpp) is involved in the uptake of essential amino acids and affects the expression of cysteine protease. *Mol. Microbiol.* **28,** 1323–1334
28. Kontinen, V. P., and Sarvas, M. (1993) The PrsA lipoprotein is essential for protein secretion in *Bacillus subtilis* and sets a limit for high-level secretion. *Mol. Microbiol.* **8,** 727–737
29. Vitikainen, M., Lappalainen, I., Seppala, R., Antelmann, H., Boer, H., Taira, S., Savilahti, H., Hecker, M., Vihinen, M., Sarvas, M., and Kontinen, V. P. (2004) Structure-function analysis of PrsA reveals roles for the parvulin-like and flanking N- and C-terminal domains in protein folding and secretion in *Bacillus subtilis*. *J. Biol. Chem.* **279,** 19302–19314
30. Ma, Y., Bryant, A. E., Salmi, D. B., Hayes-Schroer, S. M., McIndoo, E., Aldape, M. J., and Stevens, D. L. (2006) Identification and characterization of bicistronic speB and prsA gene expression in the group A *Streptococcus*. *J. Bacteriol.* **188,** 7626–7634
31. Hirano, T., Minamino, T., and Macnab, R. M. (2001) The role in flagellar rod assembly of the N-terminal domain of *Salmonella* FlgJ, a flagellum-specific muramidase. *J. Mol. Biol.* **312,** 359–369
32. Banks, D. J., Porcella, S. F., Barbian, K. D., Beres, S. B., Philips, L. E., Voyich, J. M., DeLeo, F. R., Martin, J. M., Somerville, G. A., and Musser, J. M. (2004) Progress toward characterization of the group A *Streptococcus* metagenome: complete genome sequence of a macrolide-resistant serotype M6 strain. *J. Infect. Dis.* **190,** 727–738
33. Beres, S. B., Sylva, G. L., Barbian, K. D., Lei, B., Hoff, J. S., Mammarella, N. D., Liu, M. Y., Smoot, J. C., Porcella, S. F., Parkins, L. D., Campbell, D. S., Smith, T. M., McCormick, J. K., Leung, D. Y., Schlievert, P. M., and Musser, J. M. (2002) Genome sequence of a serotype M3 strain of group A *Streptococcus*: Phage-encoded toxins, the high-virulence phenotype, and clone emergence. *Proc. Natl. Acad. Sci. U.S.A.* **99,** 10078–10083
34. Proft, T., Arcus, V. L., Handley, V., Baker, E. N., and Fraser, J. D. (2001) Immunological and biochemical characterization of streptococcal pyrogenic exotoxins I and J (SPE-I and SPE-J) from *Streptococcus pyogenes*. *J. Immunol.* **166,** 6711–6719
35. Margarit, I., Bonacci, S., Pietrocola, G., Rindi, S., Ghezzo, C., Bombaci, M., Nardi-Dei, V., Grifantini, R., Speziale, P., and Grandi, G. (2009) Capturing host-pathogen interactions by protein microarrays: Identification of novel streptococcal proteins binding to human fibronectin, fibrinogen, and C4BP. *FASEB J.* **23,** 3100–3112
36. Brouillard, J. N., Günther, S., Varma, A. K., Gryski, I., Herfst, C. A., Rahman, A. K., Leung, D. Y., Schlievert, P. M., Madrenas, J., Sundberg, E. J., and McCormick, J. K. (2007) Crystal structure of the streptococcal superantigen SpeI and functional role of a novel loop domain in T cell activation by group V superantigens. *J. Mol. Biol.* **367,** 925–934
37. Desrosiers, D. C., Sun, Y. C., Zaidi, A. A., Eggers, C. H., Cox, D. L., and Radolf, J. D. (2007) The general transition metal (Tro) and Zn2+ (Znu) transporters in *Treponema pallidum*: Analysis of metal specificities and expression profiles. *Mol. Microbiol.* **65,** 137–152
38. Nassar, N., Horn, G., Herrmann, C., Block, C., Janknecht, R., and Wittinghofer, A. (1996) Ras/Rap effector specificity determined by charge reversal. *Nat. Struct. Biol.* **3,** 723–729
39. Cole, R. M., and Hahn, J. J. (1962) Cell wall replication in *Streptococcus pyogenes*. *Science* **135,** 722–724
40. Swanson, J., Hsu, K. C., and Gotschlich, E. C. (1969) Electron microscopic studies on streptococci: I. M antigen. *J. Exp. Med.* **130,** 1063–1091
41. Carlsson, F., Stålhammar-Carlemalm, M., Flärdh, K., Sandin, C., Carlemalm, E., and Lindahl, G. (2006) Signal sequence directs localized secretion of bacterial surface proteins. *Nature* **442,** 943–946
42. Söderberg, O., Leuchowius, K. J., Gullberg, M., Jarvius, M., Weibrecht, I., Larsson, L. G., and Landegren, U. (2008) Characterizing proteins and their interactions in cells and tissues using the in situ proximity ligation assay. *Methods* **45,** 227–232
43. Virtaneva, K., Graham, M. R., Porcella, S. F., Hoe, N. P., Su, H., Graviss, E. A., Gardner, T. J., Allison, J. E., Lemon, W. J., Bailey, J. R., Parnell, M. J., and Musser, J. M. (2003) Group A *Streptococcus* gene expression in humans and cynomolgus macaques with acute pharyngitis. *Infect. Immun.* **71,** 2199–2207
44. Bushell, K. M., Söllner, C., Schuster-Boeckler, B., Bateman, A., and Wright, G. J. (2008) Large-scale screening for novel low-affinity extracellular protein interactions. *Genome Res.* **18,** 622–630
45. Rosch, J., and Caparon, M. (2004) A microdomain for protein secretion in Gram-positive bacteria. *Science* **304,** 1513–1515
46. Sarvas, M., Harwood, C. R., Bron, S., and van Dijl, J. M. (2004) Post-translocational folding of secretory proteins in Gram-positive bacteria. *Biochim. Biophys. Acta* **1694,** 311–327
47. Cole, J. N., Aquilina, J. A., Hains, P. G., Henningham, A., Sriprakash, K. S., Caparon, M. G., Nizet, V., Kotb, M., Cordwell, S. J., Djordjevic, S. P., and Walker, M. J. (2007) Role of group A *Streptococcus* HtrA in the maturation of SpeB protease. *Proteomics* **7,** 4488–4498
48. Chandra, B. R., Yogavel, M., and Sharma, A. (2007) Structural analysis of ABC-family periplasmic zinc binding protein provides new insights into mechanism of ligand uptake and release. *J. Mol. Biol.* **367,** 970–982
49. Foote, J. W., and Delves, H. T. (1984) Albumin bound and α2-macroglobulin bound zinc concentrations in the sera of healthy adults. *J. Clin. Pathol.* **37,** 1050–1054
50. Raymond, K. N., Dertz, E. A., and Kim, S. S. (2003) Enterobactin: An archetype for microbial iron transport. *Proc. Natl. Acad. Sci. U.S.A.* **100,** 3584–3588
51. Ma, Z., Jacobsen, F. E., and Giedroc, D. P. (2009) Coordination chemistry of bacterial metal transport and sensing. *Chem. Rev.* **109,** 4644–4681
52. Shannon, P., Markiel, A., Ozier, O., Baliga, N. S., Wang, J. T., Ramage, D., Amin, N., Schwikowski, B., and Ideker, T. (2003) Cytoscape: A software environment for integrated models of biomolecular interaction networks. *Genome Res.* **13,** 2498–2504
53. Lei, B., Liu, M., Chesney, G. L., and Musser, J. M. (2004) Identification of new candidate vaccine antigens made by *Streptococcus pyogenes*: Purification and characterization of 16 putative extracellular lipoproteins. *J. Infect. Dis.* **189,** 79–89

In order to cite this article properly, please include all of the following information: Galeotti, C. L., Bove, E., Pezzicoli, A., Nogarotto, R., Norais, N., Pileri, S., Lelli, B., Falugi, F., Balloni, S., Tedde, V., Chiarot, E., Bombaci, M., Soriani, M., Bracci, L., Grandi, G., and Grifantini, R. (2012) Surface Interactome in *Streptococcus pyogenes*. *Mol. Cell. Proteomics* 11(4):M111.015206. DOI: 10.1074/mcp.M111.015206.